Trends of planet formation through chemical analysis of protoplanetary disks

Colin Michael Grace

Under supervision of Dr. Ilsedore Cleeves

December 2024

Department of Astronomy

University of Virginia

This Thesis is Submitted in Partial Completion of the Requirements of BA Astronomy Major

Abstract

Our solar system's formation, as well as the formation of exoplanetary systems, may be able to be better explained by studying young stars with disks within young (1-5 Myr) star forming regions, such as Lupus, Rho Ophiucus, and Chameleon 1. Data of ^{13}CO, $C^{18}O$, C_2H, and N_2H+ were taken using the Atacama Large Millimeter Array (ALMA) at radio wavelengths, where the detection statistics among the twenty disks for each region was analyzed in relationship with various factors including the disk radial size, the effective temperature of their star, as well as the spatial distribution within a star forming region. Within this, extended disks were more likely to have detections of molecular emission than disks that solely had stars with effective temperatures above K7, while disks that were both extended and had stars hotter than K7 had the most positively identified species. Subregions in Lupus, Rho Ophiuchus, and Chameleon 1 with a higher disk density also generally had more chemical detections attributed to those disks. Separate trends in chemical detections appeared for Lupus and Chameleon 1, and Rho Ophiucus respectively. Lupus and Chameleon one both had appreciable amounts of N_2H+ and C_2H, suggesting that both CO freeze out had occurred and that there were other hydrocarbon particles, where this abundance of particles suggest that the disks of both of these regions are past the initial stages of planetary formation. Rho Ophiucus, however, lacks N_2H^+ data, and almost every single disk has ^{13}CO and $C^{18}O$ present within them, with little C_2H, suggesting that the disks of this region are still in initial stages of planetary formation.

Introduction

Our solar system formed roughly 4.5 Gyr ago, coalescing from a protoplanetary disk composed of thousands of planetesimals, into the 8 planets, various dwarf planets, and innumerable among ot asteroids and comets known today. Our understanding of the formation of our Solar System has changed over time as well, where the simple Geocentric view was dominant in earlier times, expanding out to the current Heliocentric, slightly elliptical view. Along with this, the planets of our solar system are not perfect discs of light as what was once thought, but contain their own uniqueness and unsolved statutes, whether it be the origins of Triton or the abundance of water within Jupiter. Likewise, when planets that existed beyond our Sun's gravitational influence were first detected near the turn of the millennium, a similar model of planetary formation was also applied. However, many exoplanetary systems defy this format, with various masses and radii found in the most extreme of orbits, casting our system as outliers in the galactic neighborhood. Along with this, their compositions vary widely in comparison to the silicates inner worlds and hydrogenated outer worlds of our solar system, having the most peculiar of abundances. These compositions, however, can be further explained through the chemical makeup of their building blocks, where slight abundances and deficiencies within their protoplanetary disks can lead to the most profound of changes in the planets chemically, washing away the notion that, just as our ancestors held, that these bodies are just perfect, mundane pinpricks of light in the sky. However, their chemical facets are far more complex and less understood than their 3-dimensional statutes, despite decades of study.

Even with some mystery and questions surrounding the various compositions of disks that may eventually become planets, decades of study has granted the contemporary view of chemical compositions of these disks a far wider breadth. In particular, there have been over hundreds of molecules detected in the Interstellar Medium and disks, being around 241 (McGuire 2021) composed of over a dozen elements. These elements are majorly Carbon, Hydrogen, Oxygen, and Nitrogen, with three out of the four hailing from local stellar events, such as Asymptotic Giant Branch Stars shedding their outer layers as well as nearby Supernova, all of which enrich the disks not just with these select elements, but trace elements as well. Likewise, although the majority of molecules detected are diatomic or triatomic, species with 4 or more atoms have also been detected, ranging from simple organic molecules to Carbon Buckyballs. In more recent times, however, there has been an uptick in the amount of ring-bearing molecules discovered, doubling during the time period of 2018-2021 (McGuire 2021). Along with these far larger molecules being detected in more recent times, molecules that are essentially unheard of in nature, although some can be synthesized and detected in the laboratory However, there are some far more exotic diatomics that would not be purported to have formed, given an general understanding of reactivity among the elements. The most notable of these are Noble Gas hydrides, such as ArH^+ (McGuire 2021), where the previously mentioned stellar process could be imparting effects to these atoms, allowing them to form such a exotic molecules that cannot be found here on Earth. What is more normal, regarding the species of the Interstellar Medium and, by extension, disks, is the most common ion, being cations, as cosmic rays, along with the stellar events, can cause these species to be excited, losing electrons in the process. However, there are few known anionic species, one such being NC^-. The various processes that occur in the Interstellar Medium as well as disks can impact the chemistry of said disk in far more ways than discussed here. One such notable process is the relationship revolving around CO and N_2H^+. Within this relationship, in regions dominated by CO, N_2H^+ cannot readily form, as it quickly reacts and loses that proton, becoming Nitrogen gas. However, when the CO is not present in appreciable quantities, the N_2H^+ in the disk can remain intact and become easily detectable. This behavior, as well as the abundances of a few other select molecules, have been scrutinized further by the study of about 80 disks conducted as part of the ALMA Cycle 9 Large Program “The Disk-Exoplanet C/Onnection” (DECO).

DECO surveyed dozens of molecules, ranging from simple carbon chains to sulfur-bearing species and simple organics, such as Formaldehyde. The sample was split up into four groups, with twenty hailing from each of the Lupus, Rho Ophiuchus, Taurus, and Chameleon 1 star forming regions. In the present thesis, I focus on the commonly observed molecules ^{13}CO, $C^{18}O$, C_2H, and N_2H^+. Despite the analysis of only four molecules over a span of 80 disks, they provide a representative view of the chemistry of other disks in similar low mass star forming environments and thus can be used as a representative sample for other protoplanetary disks. Within this, the relationship between ^{13}CO and N_2H^+ can be examined for disks within a similar environment, and potentially be put into context with other disks that are placed in more active star-forming environments, where the physical conditions could be different but the same molecular astrophysics applies. Essentially, the disks sampled as part of DECO can act as a baseline for what would be considered normal rates of N_2H^+ prevalence.

The DECO survey was conducted with the intent to analyze the chemical compositions of various protoplanetary disks, looking for key molecules, such as N_2H^+ and isotopes of CO. This survey has been proposed at this time in particular to capitalize on the sensitivity of ALMA, allowing rapid detections of many sources quickly at moderate spatial resolution. Along with this, the recently launched and relatively unharmed by micrometeoroid impacts James Webb Telescope is fully operational, which can reveal molecular emission at infrared wavelengths. Thus, with both of these instruments utilized on the same disk, the chemical story of the protoplanetary disk could be written more completely, and with a far higher accuracy. Such as applying a cm radio observation of a cold dark cloud (McGuire 2021) and an infrared observation to determine why some molecules appear in a significant abundance, as the background starlight could ionize them, allowing for other chemical reactions to occur.

Methods

In order to properly compare the chemical detections of ^{13}CO, $C^{18}O$, C_2H, and N_2H^+, each of the disks had to be observed with ALMA using Bands 6 and 7. These observations totalled approximately 150 hours of observatory time, including overheads. The spectra were obtained for ^{13}CO and $C^{18}O$ at 220.399 GHz, 219.56 GHz respectively. C_2H was observed at 262.004 GHz, 262.006 GHz, 262.005 GHz, and 262.007 GHz. N_2H^+ was also observed at 279.512 GHz. Along with this, the rotational transitions that were observed at these frequencies were, for C_2H, 3-2, 3-2 for N_2H^+, and 2-1 for ^{13}CO and $C^{18}O$. However, at the time of the writing of this thesis there was not a truly complete set of data. This is most notable with the absence of N_2H^+ from the channel maps of Rho Ophiuchus. Although N_2D^+ was part of the spectral setup, its binning did not result in clear detections substantial for major analysis. This can be extended to some other disks, where, in Lupus, disks Sz 75 and Sz 77 both were missing ^{13}CO and $C^{18}O$. In Chameleon 1, disks with DECO names of J11100469-7635452 and J11081509-7733531 were both missing ^{13}CO and $C^{18}O$. For this thesis, I fit all existing detections available in mid-Fall 2024.

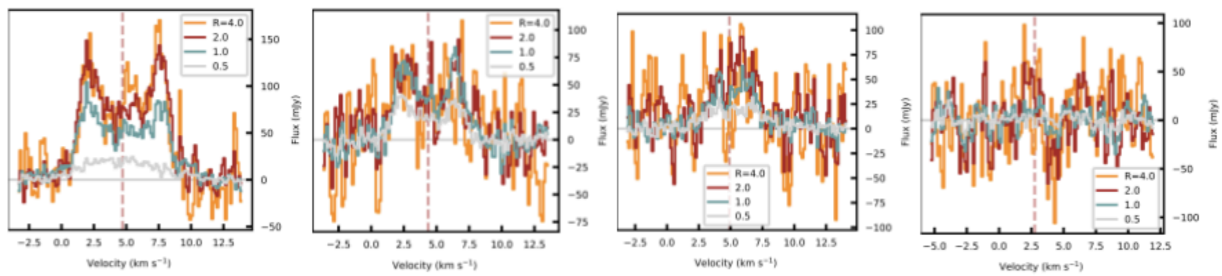

Figure 1: Classification of the detection types within the regions' disks. The different colors signify different aperture sizes in arcseconds. From left to right: Classical Keplerian double-peaked profile, Classical Keplerian shallow double-peaked profile, single broad peak, and no clear detection (potential weak components, but not obvious in all four apertures).

The detections were classified on whether or not they fit the classical absorption pattern of an orbiting Keplerian disk, where the central absorption peak can be deep or shallow, or a single broad peak pattern, with a negative detention being pure noise as per Figure 1. Despite this lack of certain channel maps, the detections, as well as their distances from the Solar System, in parsecs, were graphed through python-based code developed as part of the UVA thesis of Margaret Haun (2024), where each of the chemicals within a specific disk were separated and plotted with their detection status indicated by different colors, accomplished through binary delimiters, as well as a third delimiter in case the chemical did not have any channel maps in a particular disk(s). Along with this, the distances of the disk to our Solar system were standardized and made accurate through other algorithms (Haun, UVA Thesis, 2024), where their true positions are given. All three regions of 20 disks each were separately graphed, where all 3 of them use nearly identical code, although some delimiters had to be changed, as different regions had some chemicals that were not present, while others did have them present throughout all 20 disks. Similarly, I graphed detections in relation to whether the disk orbited a solar-mass or lower mass star or if the disk itself was radially extended, denoted by separate colors in a bar format, not taking into account position.

Findings

Lupus

Lupus is a consortium of molecular clouds, being about 200 parsecs away from our Solar System (Comerón 2008). Thus, it is one of the closest star forming regions to our sun, and is majorly composed of four regions of star formation. These regions are composed of various highly active T Tauri stars, such as RU Lup, as well as pre-main sequence M type dwarfs (Comerón 2008). Along with this, it is one of the larger mass star forming regions relatively close to the sun in both angular size and mass, similar to other star-forming regions within roughly 200 parsecs. The development of the complexes within Lupus was likely shaped by the Scorpius-Centaurus OB association (Comerón 2008) and its relatively high Ultraviolet emission.

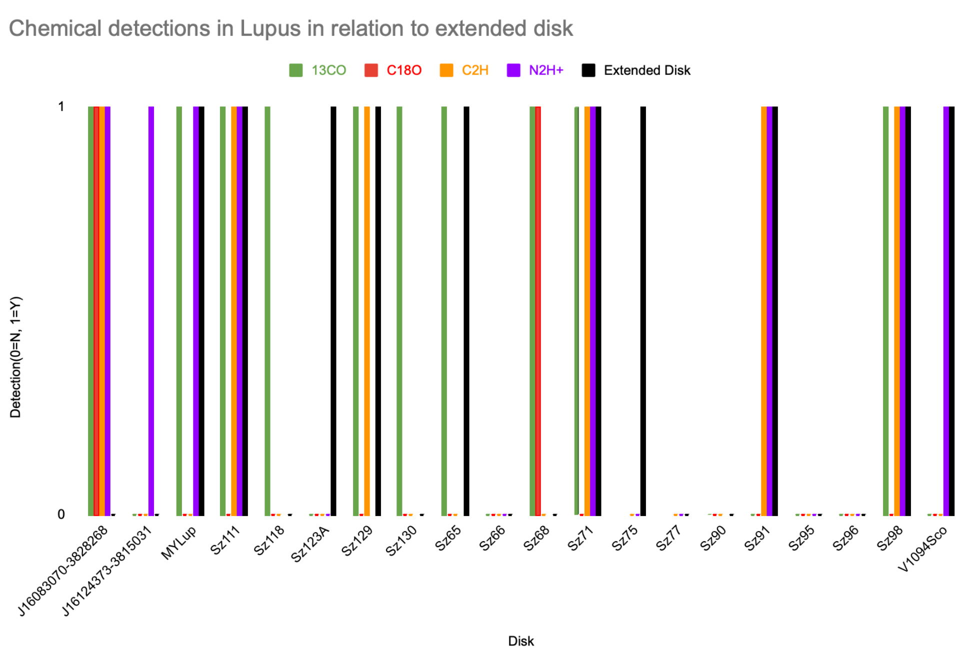

Figure 2: Per disk detections for the Lupus sample compared to the disk radial size (extended).

Within DECO's observations of Lupus, a variety of chemical detections have been denoted across almost all twenty disks. As per Figure 2, they have a greater range and variety. Within this, almost every single extended disk in Lupus has at least one chemical detection, with ^{13}CO and N_2H^+ being the most commonly detected molecules within these disks. However, there are some disks that defy this overall characterization. This is most notable with Sz 75, Sz 132A, and, especially J16083070-3828268. With Sz 75 and Sz 132A, despite their status as extended disks, they do not have any detections of ^{13}CO, $C^{18}O$, C_2H, or N_2H^+. On the opposite side of the chemical detection intensity is J16083070-3828268, where, despite not being extended, it presents all four molecules, also being the only disk to have all four detections simultaneously. Despite these trends, examining the effective temperature of the disk's host star can give insight into the detection statistics.

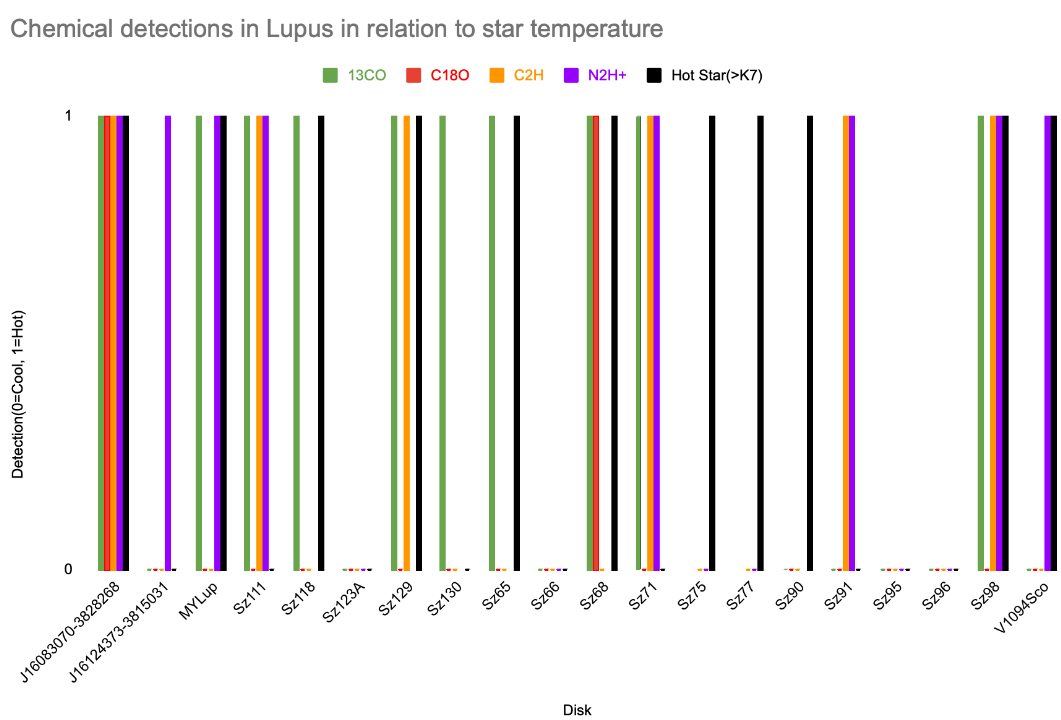

Figure 3: The detections in Lupus compared to the star's effective temperature (>K7).

With Figure 3, the stellar conditions of the disks are analyzed, in particular, the boundary between sub K7 and K7 and above stars. However, unlike the disk extension, there is a lesser correlation between detections and star temperature. Within this, only 72% of all disks with stars hotter than K7 have detentions of ^{13}CO, $C^{18}O$, C_2H, and N_2H^+. The most common detection in these disks, despite this, is ^{13}CO, with N_2H^+ being somewhat less detected. This trend of absence is most noticeable with Sz75, Sz77, and Sz90, where, despite their disks surrounding a star >K7, they have no directions whatsoever. One disk in particular that upsets this trend is J16083070-3828268, where its disk has all chemical detections noted within it.

Overall, the chemical detections in Lupus favor a more extended disk than having a central star more luminous than K7, but there are some disks that indeed usurp this trend in both detection amount and type, such as N_2H^+ being more common with extended disks, and ^{13}CO being more common in relation to disks with hotter stars.

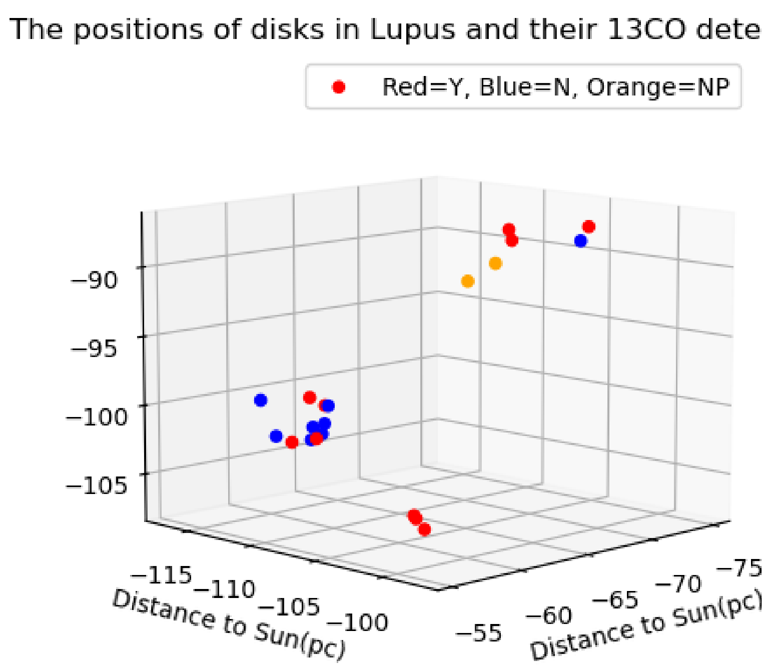

Figure 4: Spatial distribution of disks in Lupus with ^{13}CO detections.

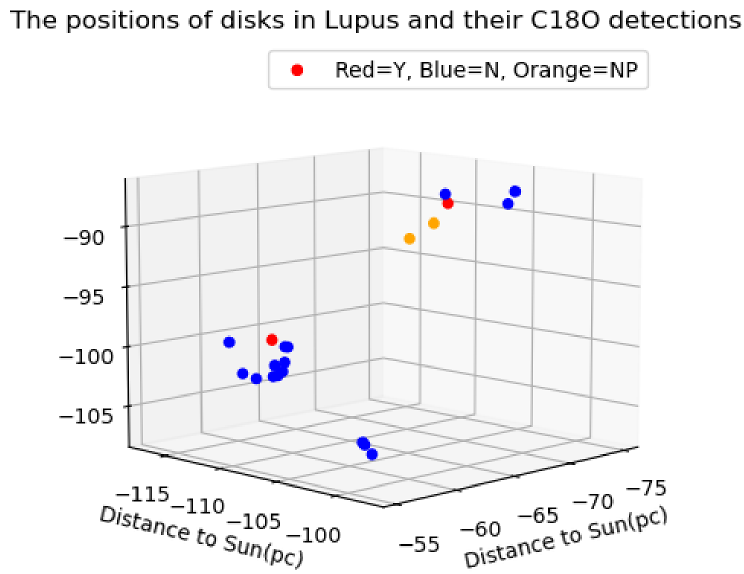

Figure 5: Spatial distribution of disks in Lupus with $C^{18}O$ detections.

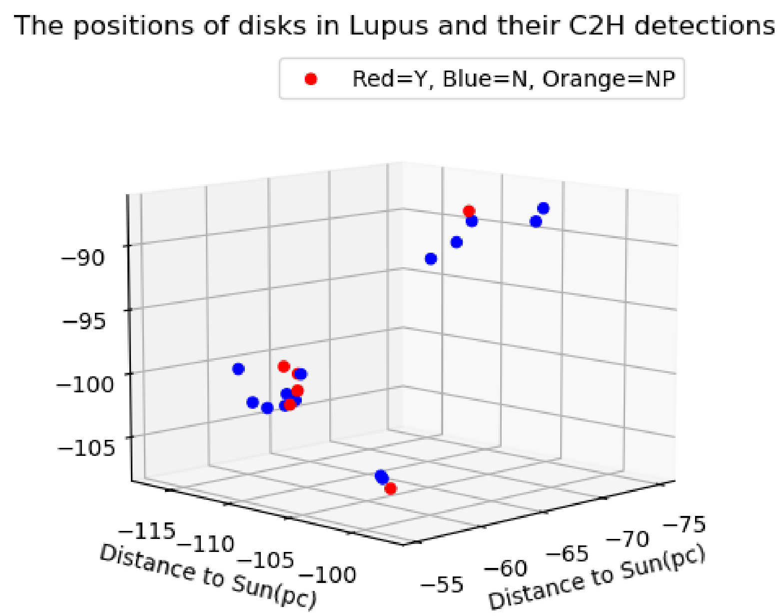

Figure 5: Spatial distribution of disks in Lupus with C_2H detections.

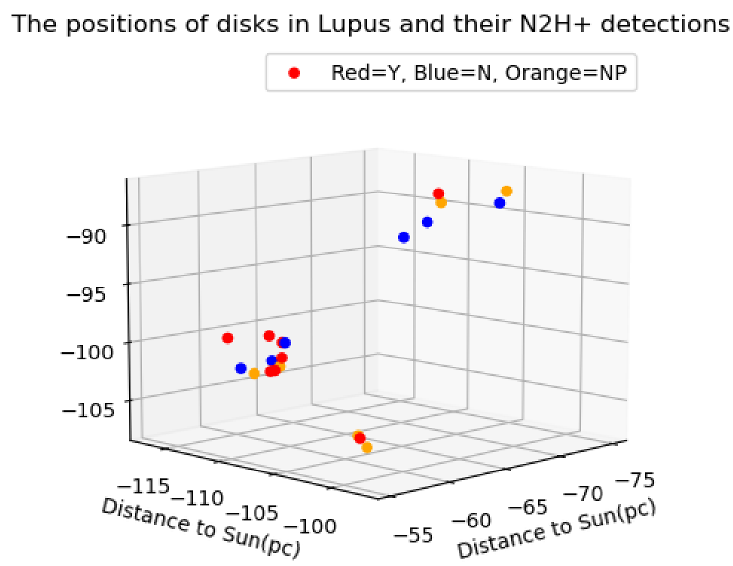

Figure 7: Spatial distribution of disks in Lupus with N_2H^+ detections.

The detections of ^{13}CO, $C^{18}O$, C_2H, and N_2H^+ have also been correlated with certain structures within the spatial positions of disks within Lupus. This is most evident with the assembly of disks in a relatively populated region, seen toward the lower left of Figures 4, 5, 6, and 7. All four molecules have been detected in this structure, although their relative detections differ somewhat. This is most notable with $C^{18}O$, where it has only been detected within this assembly once, with the other detection lying in a smaller assembly of disks to the upper right of Figures 4, 5, 6, and 7. Another small region comprising three disks to the bottom center of Figures 4, 5, 6, and 7 display ^{13}CO in all three, while not presenting $C^{18}O$ at all. Two molecules that have been present in all three subregions are C_2H and N_2H^+, where C_2H more heavily populated the lower left region, similar to ^{13}CO, but defies the trends of the other molecules by having its detections more evenly distributed among the three subregions. This trend continues with N_2H^+, being the most detected molecule in Lupus, being more present in all three subregions in comparison to ^{13}CO, which had a concentration in the lower center subregion.

Overall, these spatial graphs demonstrate that the majority of the molecules have higher rates of detection in regions with a higher density of disks, although, for some disks, ^{13}CO, $C^{18}O$, and N_2H^+ did not have any data attributed to them, so this trend may change as more data is collected.

Rho Ophiuchus

Rho Ophiuchus is a star forming region about 165 parsecs away from our Solar system and has a mass somewhat greater than 2000 Solar Masses (Klose 1986). Thus, in comparison to clouds that are slightly farther away, a great amount of spectroscopic data has been collected. This has resulted in determining that, through X-Rays, this region is not interacting with supernova remnants or a neutron star (Klose 1986). Along with this, towards the center of the cloud, there is a cluster of roughly 50 stars, and the cloud in total only contains about 3 B-type Supergiants (Klose 1986), both analyzed via Infrared. Likewise, the average temperature of dust reaches about 50 K (Klose 1986).

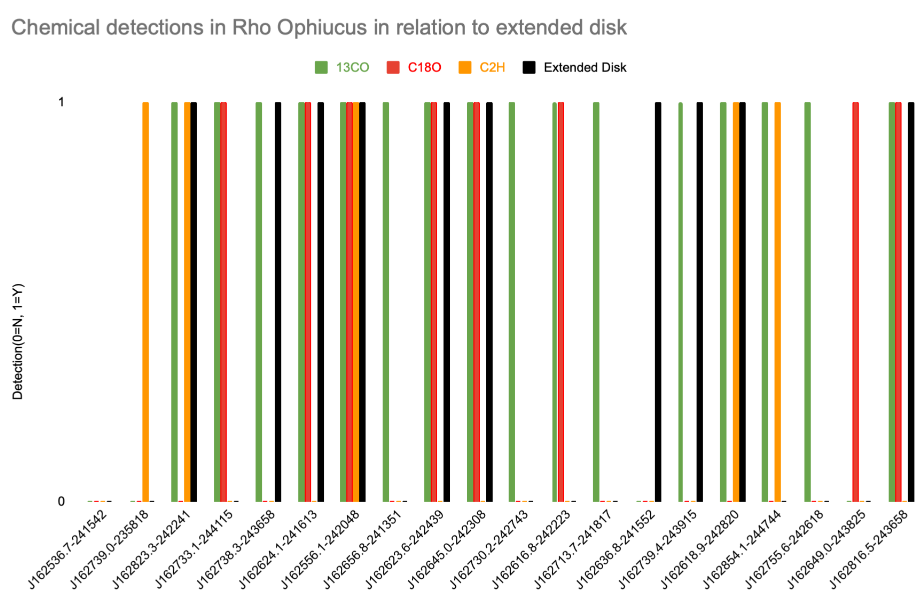

Figure 8: The detections in Rho Ophiuchus compared to the disk extension

Within Rho Ophiuchus, the variety of chemical detentions is significantly less than the four chemicals detected, although the amount of detections themselves have increased among certain molecules. In terms of extended disks with Figure 8, there are substantially more detections within them in comparison to disks with a relatively hot star, with ^{13}CO being present in the majority of disks, regardless of their status as extended or having a star hotter than K7. $C^{18}O$ is also present in a significant amount, with C_2H trailing somewhat in detections. Extended disks also have higher rates of detections especially with $C^{18}O$ and C_2H.

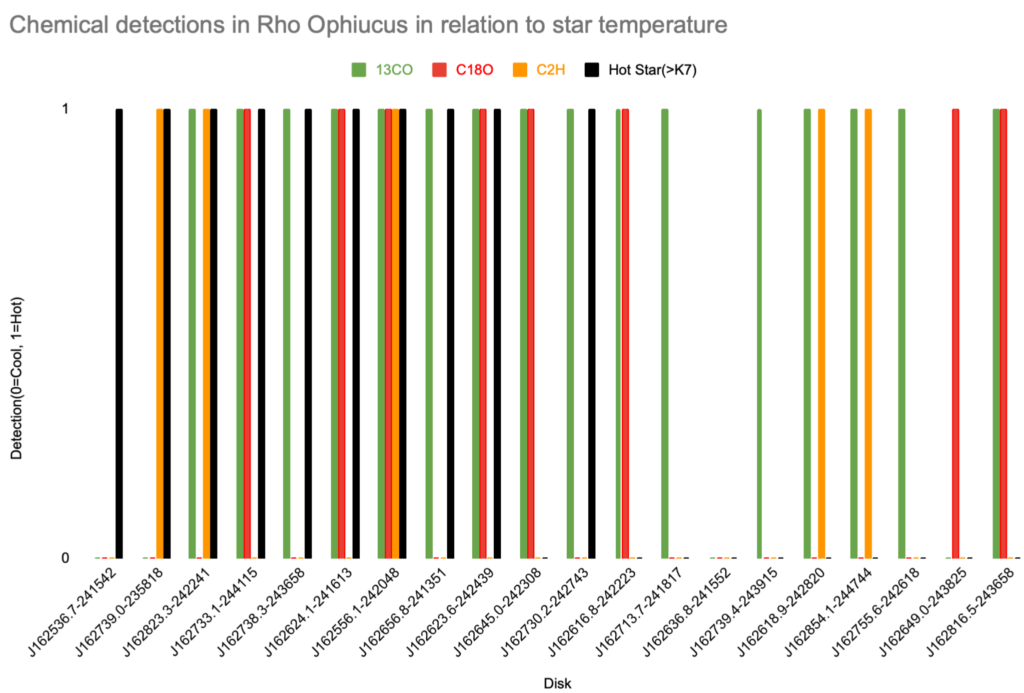

Figure 9: The detections in Rho Ophiuchus compared to stellar temperature(>K7)

In terms of disks with stars hotter than K7 as per Figure 9, however, there are slightly fewer chemical detections in relation to disk extension, where disks that have stars above K7 have a substantial amount of detections, although fewer in number than their extended counterparts. However, one major feature of Rho Ophiucus to note is that, with disks that are both extended and have stars hotter than K7, they have a significant majority, if not all molecules detected within them, most notable with J162556.1-242048 and other disks. Along with this, the range of chemical detections is less concentrated to just strictly extended or stars above K7, as, although extended have more detections as previously mentioned, there is not a significant difference between the amount of detections in disks with stars hotter than K7 and extended disks, as both variety demonstrate all three chemical detections.

Overall, although extended disks generally have more detections, they are not as dominant in terms of such in comparison to disks with stars above K7. Thus, the amount of detections is more blended, where some molecules are far more dominant than others despite higher amounts of detections overall, such as with ^{13}CO. However, unlike ^{13}CO and $C^{18}O$, C_2H was detected more so in disks that were both extended and had stars hotter than K7.

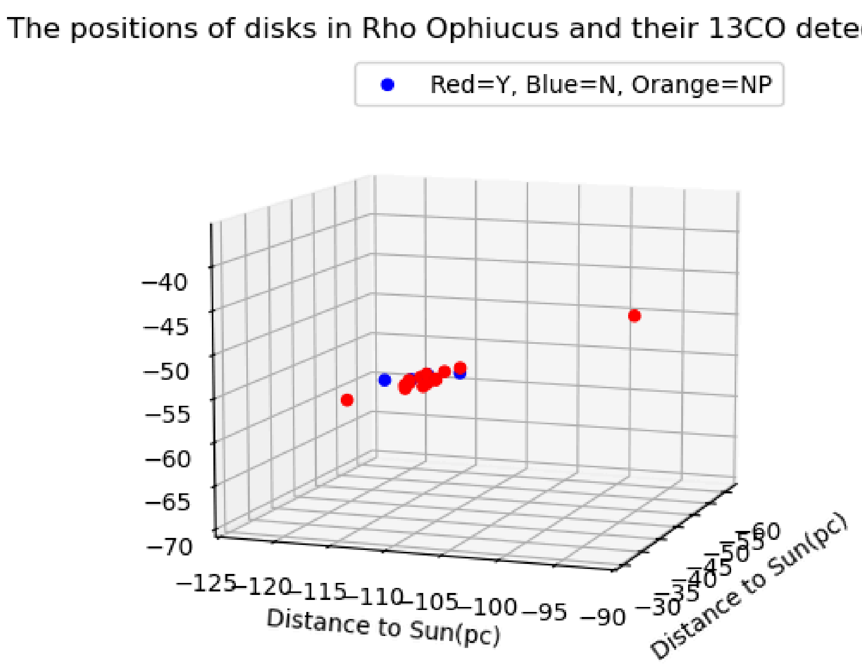

Figure 10: Spatial graphing of disks in Rho Ophiuchus with ^{13}CO detections

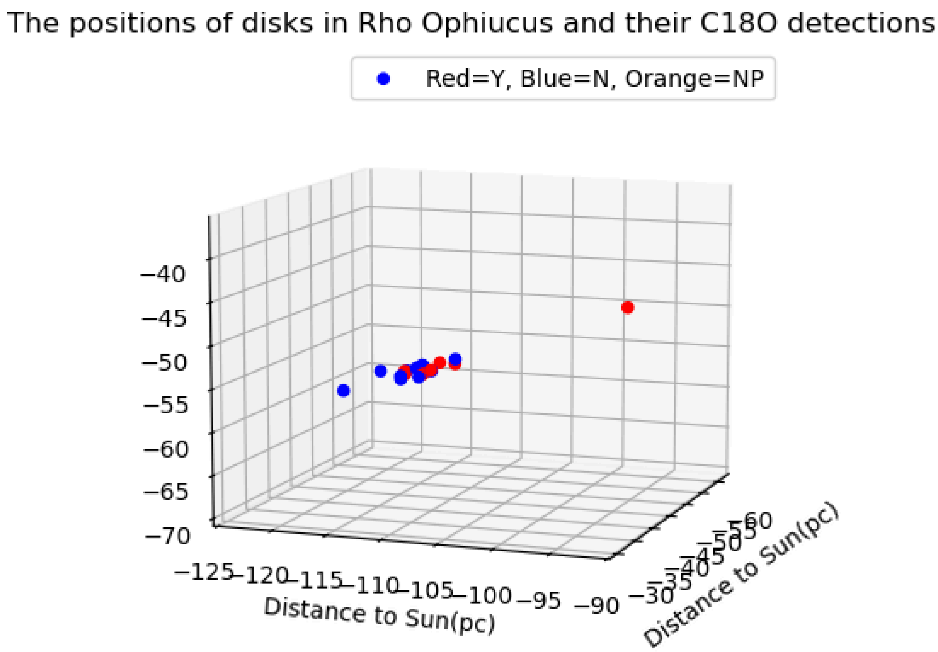

Figure 11: Spatial graphing of disks in Rho Ophiuchus with $C^{18}O$ detections

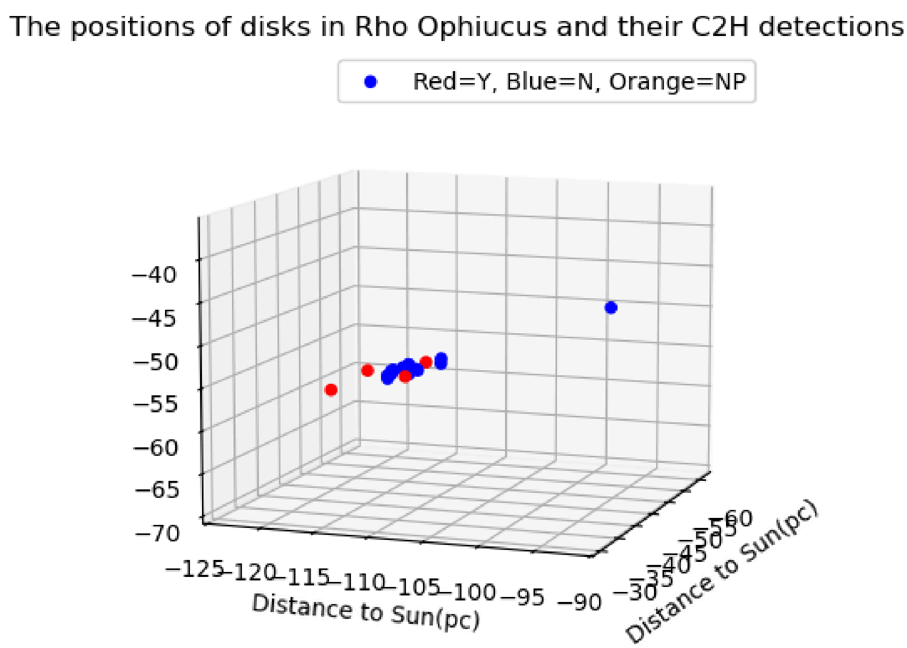

Figure 12: Spatial graphing of disks in Rho Ophiuchus with C_2H detections

In terms of spatial arrangement, Rho Ophiucus appears to have a single, dense region of disks concentrated within the center of the graphed region, with three major outliers, one significantly farther away from the rest. With ^{13}CO as per Figure 10, it was detected almost universally across all the disks, including the three outliers outside this dense region. This trend of detections within the densest region of disks is continued slightly less so with Figure 11 and $C^{18}O$, where unlike ^{13}CO's almost universal detection, $C^{18}O$ appeared closer to the center of the region of highest disk density. Nonetheless, it was also detected in the farthest outlier. With C_2H as per Figure 12, however, this trend of higher detections in regions of higher disk density is not seen, as C_2H is detected in the pair of disks to the left of the densest region, and only detected twice within the densest region. These results were compounded by C_2H having a lower rate of detection overall in comparison to ^{13}CO and $C^{18}O$. C_2H also does not appear to be detected within the most crowded portions of the central dense region, instead being on the borders of this consortium of disks.

Overall, in terms of spatial arrangement, ^{13}CO was detected almost universally, while $C^{18}O$ followed this trend, although with a slightly lower amount of detections. C_2H defies this trend set by ^{13}CO and $C^{18}O$ significantly, only appearing on the border of the dense central region and the disks to the left of this region. Unfortunately, N_2H^+ was not available at the time of this thesis. Thus, for this region, it was not possible to graph either the detections in relation to disk extension or a star above K7, along with their spatial arrangements.

Chameleon 1

Chameleon 1 is a star-forming region between 160 and 180 parsecs away from the Sun (Winston et. al 2012), and is notable for forming primarily lower mass stars in comparison to more notable regions, such as Orion. Thanks to multiple spectroscopic surveys of the region, it appears that the age of the region is only about 2 Myr (Winston et. al 2012). Another major feature to note is that relatively low extinction, ranging between A_v=5 and A_v=20 (Winston et. al

2012), making the protostellar objects within relatively visible, granting a full view of the objects and disks within. This region is primarily divided into two other regions, being a Northern region and smaller Southern clusters (Winston et. al 2012).

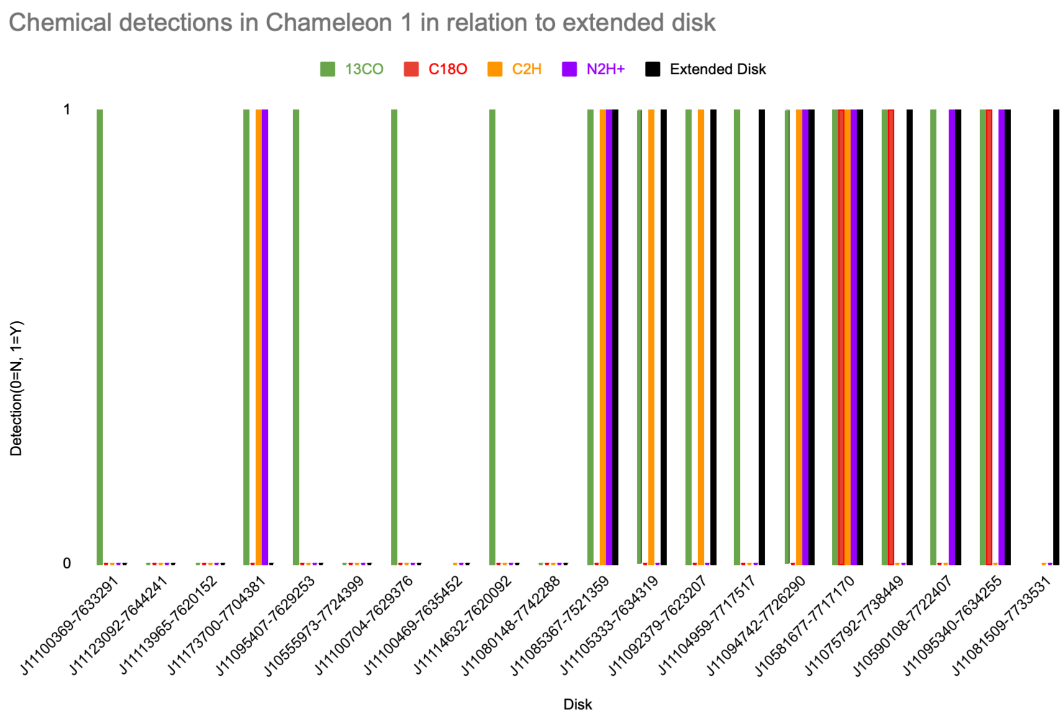

Figure 13: The detections in Chameleon 1 compared to disk extension

Within Chameleon 1, there appears to be an significant abundance of ^{13}CO present in almost all regions, along with a near complete deficit of $C^{18}O$, while C_2H and N_2H^+ are relatively evenly matched in abundance. In terms of disk extension as per Figure 13, they have a significantly high amount of detections across all molecules, with most notable molecule being correlated to disk extension being C_2H, while other molecules are more evenly spread among extended disks and disks with a relatively hot star above K7. ^{13}CO does appear within almost every extended disk, only being absent from extended disks J11100369-7633291, J11095407-7629253, J11100704-7629376, and J11114632-7620092. $C^{18}O$ does indeed appear within extended disks, but with a relatively low amount of detections in relation to the other three molecules.

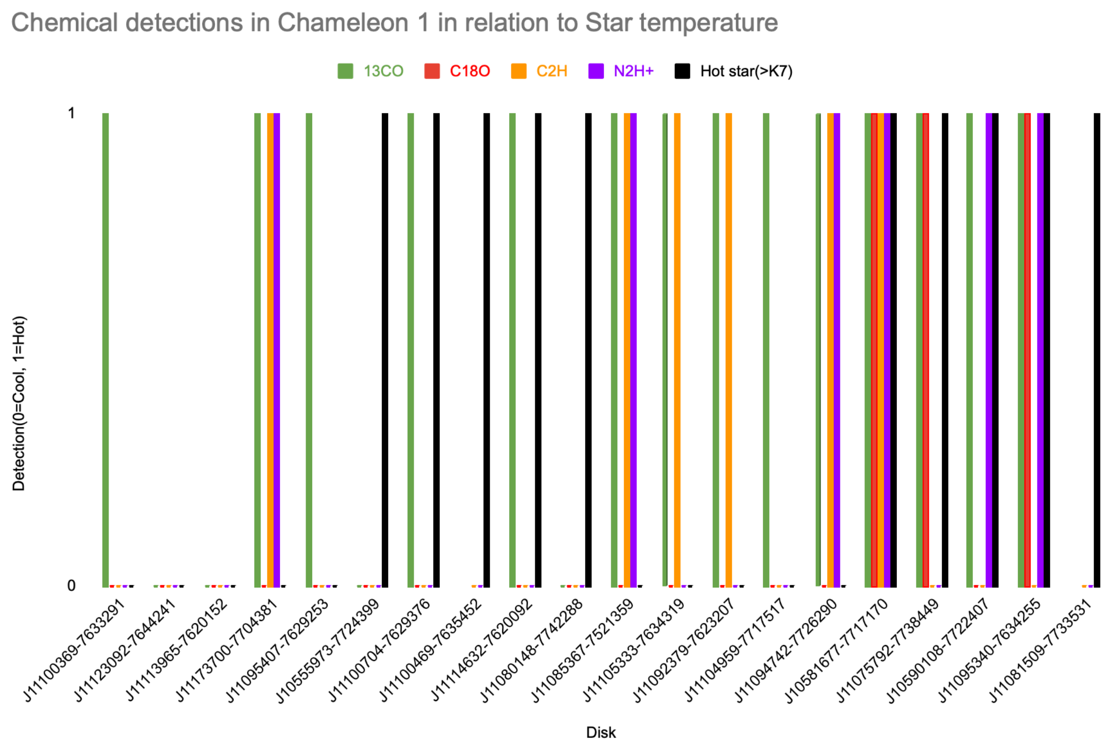

Figure 14: The detections in Chameleon 1 compared to the star temperature(>K7)

In terms of whether or not the disk has a star hotter than K7, as per Figure 14, ^{13}CO is again almost present in all of these disks, while other molecules are relatively lacking in detections within them. The most glaring molecule that is not detected within these types of disks is C_2H, only being present in one disk with a star above K7, being J10581677-7717170. With N_2H^+, it is present with an appreciable amount of detections across these regions, although less appreciable than in relation to extended disks. Similar to the extended disks, $C^{18}O$ is also detected in hot disks with identical rates of detection.

Overall, although disks that are both extended and have stars hotter than K7 have a substantial amount of chemical detections, it is the extended disks that have more detections than those that solely have stars above K7. However, $C^{18}O$ is only present within disks that are both extended and have stars hotter than K7, while ^{13}CO has the opposite trend, appearing in almost all disks.

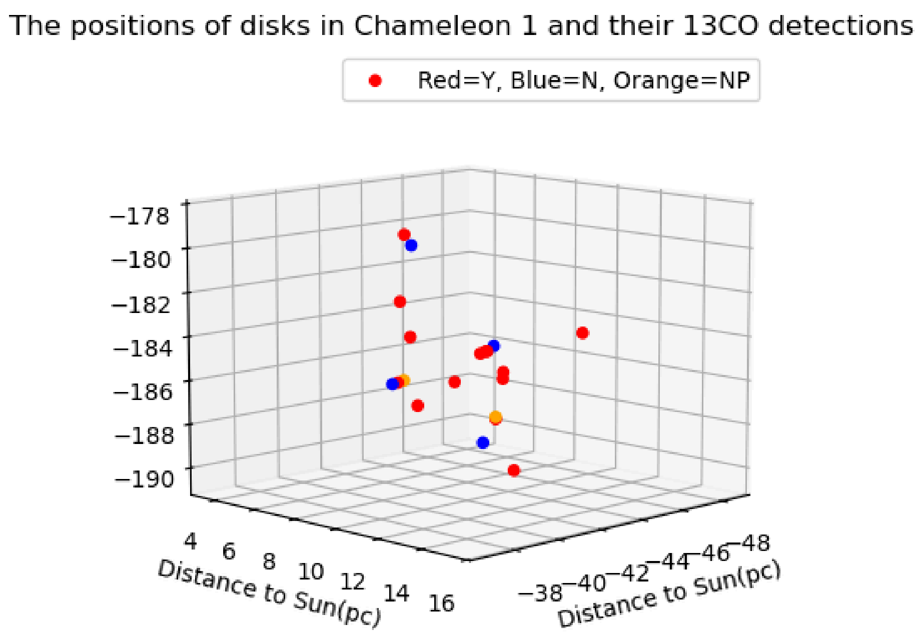

Figure 15: Spatial graphing of disks in Chameleon 1 with ^{13}CO detections

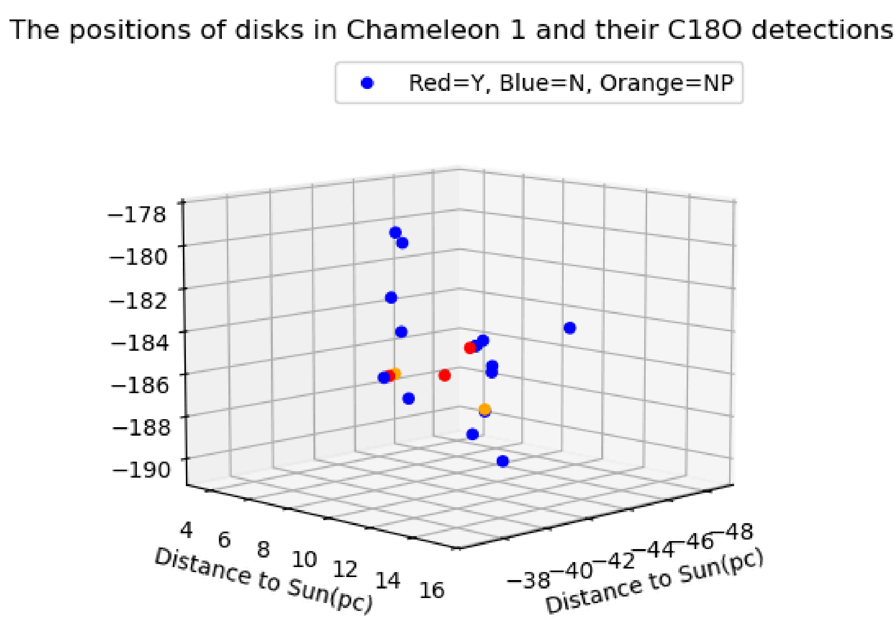

Figure 16: Spatial graphing of disks in Chameleon 1 with $C^{18}O$ detections

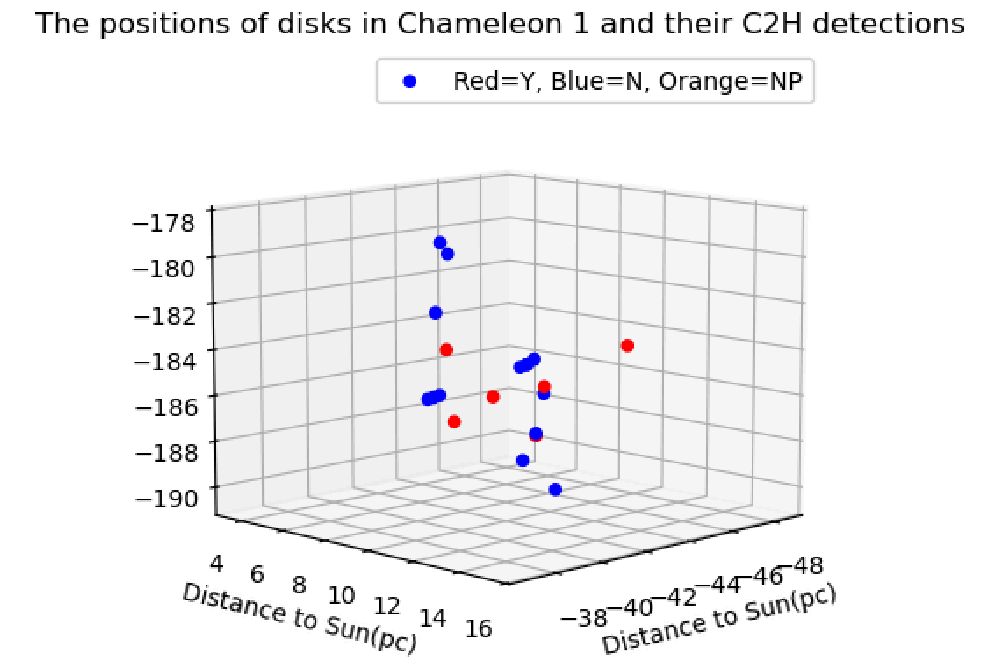

Figure 17: Spatial graphing of disks in Chameleon 1 with C_2H detections

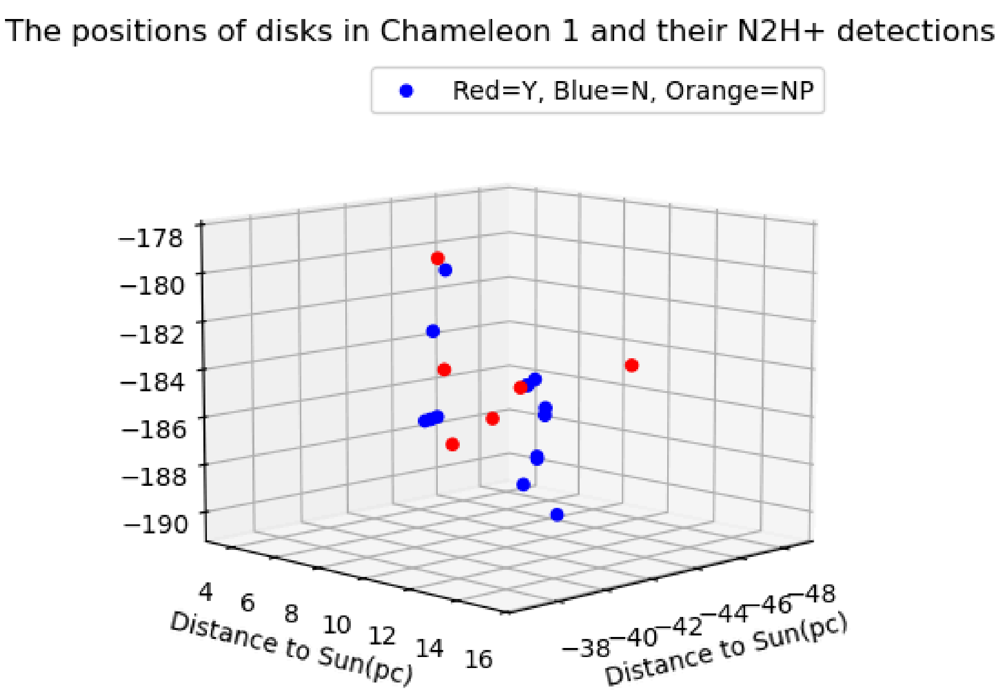

Figure 18: Spatial graphing of disks in Chameleon 1 with N_2H^+ detections

With the spatial graphing of the region, $C^{13}O$ is present within all subregions, ranging from the center portion comprising several disks, to the filaments appearing to extend outwards, as well as the one lone disk away from the rest of the larger subregion within Figure 15. On the opposite trend as ^{13}CO, $C^{18}O$ is almost entirely absent from Chameleon one, and, when it is detected within a disk, it is detected towards the center of the semi-circular subregion as per Figure 16. C_2H and N_2H^+ appear to follow similar trends to one another, being detected significantly in the central subregion, although the different filaments have different rates of detection between the molecules. With C_2H as per Figure 17, it is most commonly detected within the central subregion, as well as being detected in the outlying disk away from the rest of the subregion, with one detection in the lower filament. N_2H^+ is both similar and different in this regard with Figure 18, where, although it is detected in the central subregion just as C_2H is, it has more deletions within a filament, in particular, the upper filament. Along with this, it is also detected in the same outlying disk as C_2H was.

Overall, ^{13}CO dominates the detections in Chameleon 1 regardless of the location of the disk in relation to the others. $C^{18}O$ follows the opposite of this trend, being detected mostly within the central subregion. C_2H and N_2H^+ follow trends similar to each other, where the majority of their detections are in the central subregion, with slight differences in terms of detections within the filaments of disks branching off from this central region. However, there are two disks that did not have ^{13}CO data given, so its trend may be added to or subtracted from. Identical to ^{13}CO, it is lacking data within two disks. Thus, there may be potentially more $C^{18}O$ than is currently presented.

Conclusions

Within the regions of Lupus, Rho Ophiucus, and Chameleon 1, there are two major trends within chemical detections and thus stages of planetary formation among their disks. With these regions, they appear to follow similar trends in chemical detections in both temperature, size, and spatial distribution. In terms of temperature, disks within Lupus and Chameleon 1 that had stars that were hotter than K7 were overall not as conducive to the amount of chemical detections as was their relative extension. However, the disks that had all four molecules detected were often both extended and having a star above K7 in temperature. Thus, the boost in temperature for these disks is helpful and would contribute to potentially accelerated planetary formation thanks to the presence of these chemicals, rather than disks that were solely extended or had a star above K7. However, planetary formation overall may be more advanced in Lupus and Chameleon I due to the significant presence of N_2H^+ within both regions, signifying that the CO freeze-out has begun, and thus icy bodies could begin to form from this, growing into larger planetesimals. Along with this, C_2H is present in appreciable quantities in both regions, where these radicals could react with other molecules, also producing grains that would form planetesimals in conjunction with the CO ice. Thus, the ^{13}CO and, in particular, $C^{18}O$ abundances in both regions are somewhat lower than that of Rho Ophiuchus.

However, Rho Ophiuchus appears to follow a trend of its own in relation to chemicals detections, though analysis of this region is limited by not yet having the N_2H^+ observations imaged at the time of this thesis. . Rho Ophiucus is notable for having ^{13}CO detected in almost every single disk of the sample. Along with this, $C^{18}O$ is detected in this region at far higher rates than Lupus and Chameleon one, while C_2H seems to be relatively rare within Rho Ophiuchus. Thus, it appears that Rho Ophiucus has not had enough time for more freeze-out based processes to occur, suggesting that the amount of ices within this region is significantly lower than the other two regions, where planetary formation is in a earlier stage or is occurring at a slower rate in comparison to Lupus and Chameleon 1.

References:

Bergin, E., & Cleeves, I. (2023). Chemistry During the Gas-rich Stage of Planet Formation. *Exoplanet Handbook*. https://www.dropbox.com/scl/fi/gsg5us2b1ylug46jtg6e8/Exoplanet_Handbook__Disk_Chemistry_Version_2.pdf?rlkey=gledjhp2g4tsfyilgr5hr2dfs&e=1&dl=0

Cleeves et al. (2022). The ALMA Disk-Exoplanet C/Onnection. https://virginia.app.box.com/file/1646816181171

Comerón, F. (2008). The Lupus clouds. In *II Astronomical Society of the Pacific*. https://elt.eso.org/public/archives/releases/sciencepapers/eso1303/eso1303a.pdf

Haun, Margaret. (2024). Interpreting Spatial Distributions of ALMA DECO Sample Selections.. https://libraetd.lib.virginia.edu/public_view/dj52w6044

Klose, S. (1986). The Rho Ophiuchi cloud – An overview. *Astrophysics and Space Science*, *128*(1), 135–149. Accessed 2 December 2024. https://doi.org/10.1007/bf00656025

McGuire, B. (2021). 2021 Census of Interstellar, Circumstellar, Extragalactic, Protoplanetary Disk, and Exoplanetary Molecules. 1-55. https://arxiv.org/pdf/2109.13848

Winston, E. et al. (2012). *Herschel* Far-IR observations of the Chamaeleon molecular cloud complex. *Astronomy and Astrophysics*, *545*, A145–A145. https://doi.org/10.1051/0004-6361/201118665